Amino Acids (2011) 41:923–932
DOI 10.1007/s00726-010-0791-0

ORIGINAL ARTICLE

Proteomic analysis of apoptosis induction in human lung cancer cells by recombinant MVL

Yuqin Li · Bochao Zhang · Xiaoqin Wang · Huidan Yan · Gu Chen · Xuewu Zhang

Received: 21 August 2010 / Accepted: 15 October 2010 / Published online: 11 November 2010

Abstract Lung cancer is still difficult to treat by current chemotherapeutic procedures. We recently found that MVL, an anti-HIV lectin from blue-green algae *Microcystis viridis*, also has antitumor activity. The objective of this study was to investigate apoptosis-inducing activity of recombinant MVL (R-MVL) and proteomic changes in A549 cells, and to identify the molecular pathways responsible for the anti-cancer action of R-MVL. We found that R-MVL induces A549 cells apoptosis in a dose-dependent manner by using MTT assay, fluorescent microscope (FM) and flow cytometry (FCM), and the IC50 was calculated to be 24.12 μg/ml. Subsequently, 7 altered proteins in R-MVL-treated A549 cells were identified, including upregulated aldehyde dehydrogenase 1 and β-actin, and five downregulated proteins: heat shock protein 90, heat shock 60, plastin 3, tropomyosin 3, and β-tubulin. Further bioinformatics analysis predicted the potential pathways for R-MVL to induce apoptosis of A549 cells. In conclusion, this is the first report to investigate anti-cancer activity of R-MVL and its mechanism of action by proteomics analysis. Our observations provide potential therapeutic targets for lung cancer inhibitor intervention and implicated the development of novel anti-cancer therapeutic strategies.

Y. Li · B. Zhang · X. Wang · H. Yan · G. Chen · X. Zhang (✉)
College of Light Industry and Food Sciences,
South China University of Technology,
381 Wushan Road, Guangzhou 510640, China
e-mail: snow_dance@sina.com

Y. Li
Biotechnology Institute, College of Chemical Engineering,
Xiangtan University, Xiangtan, China

Keywords Recombinant MVL · Lung cancer · Apoptosis · Proteomics · Pathways · Bioinformatics

Introduction

Lung cancer is one of the leading causes of death worldwide (Greenlee et al. 2000). The number of lung cancer patients has been gradually increased, with 1.2 million new cases diagnosed every year and 1 million deaths being recorded in both men and women (Gridelli et al. 2003). Despite the fact that our understanding of the biology of cancer has undoubtedly improved in the last decade, lung cancer is still difficult to treat by current chemotherapeutic procedures. Thus, it is essential to define new treatment strategies and detect new therapeutic targets (Pan et al. 2008).

Microcystis viridis lectin (MVL), a mannose-binding protein, was originally isolated from aqueous extracts of the unicellular freshwater bloom-forming cyanobacterium (blue-green algae) *Microcystis viridis* NIES-102 (Yamaguchi et al. 1999). It is a 13-kDa single polypeptide containing 113 amino acid residues and possesses two highly homologous domains, each domain involved 54 amino acid and the two domains are connected by a linker consisting of 5 amino acid residues. MVL has been shown to have inhibition activity to laboratory and clinical isolates of HIV and other enveloped viruses by binding oligosaccharides on the surface of the viral envelopes (Li et al. 2008b; Williams et al. 2005). Interestingly, we recently found that MVL also has anti-cancer activity. Due to very low contents of MVL in the corresponding algal species, we successfully cloned and expressed MVL in *E. coli*, enable to obtain a large quantity of recombinant MVL required for further research.

Proteomics analysis, which usually involves a combination of two-dimensional electrophoresis (2-DE), image

analysis, and mass spectrometry identification (Kim et al. 2008), is rapidly becoming an important research area for comprehensive study of protein expression patterns under a specific set of conditions. The altered proteins identified by proteomic approach can be further characterized as potential drug targets and the global analysis of the protein variations can generate valuable information to understand cancer biology or the drug action mechanisms (Martinkova et al. 2009).

In this paper, we first investigated apoptosis induction of R-MVL in lung cancers using MTT assay, fluorescent microscopy and flow cytometry. Then, we employed a global proteomic-based approach to look for the potential mechanism of apoptosis induced by R-MVL. The protein profiles of A549 cells treated with R-MVL were compared to those untreated control, and seven differentially expressed proteins were identified, including upregulated aldehyde dehydrogenase 1 family member A1 (ALDH1A1) and β-actin (ACTB), and five downregulated proteins: heat shock protein 90 kDa beta (HSP90B1), heat shock 60 kDa protein 1 (HSPD1), plastin 3 (PLS3), tropomyosin 3 (TMP3), and β-tubulin (TUBB). Further bioinformatics analysis suggested that 14-3-3 zeta or 14-3-3 beta could play very important role in MVL-induced apoptosis in A549 cells, and R-MVL might follow three potential pathways to induce apoptosis of A549 cells: CHUK—NFKBI—NFKB—TRAF—apoptosis or MDM2—p53—apoptosis or AR—PSA—apoptosis. This provides potential therapeutic targets for lung cancer inhibitor intervention and direct implications for the development of novel anti-lung cancer therapeutic strategies.

Materials and methods

Materials

A549 cell line was purchased from the people hospital of Guangdong province (Guangzhou, China). RPMI-1640 media was obtained from GIBCO (Grand Island, NY, USA). Glycerol, thiourea, and trypsin (sequencing grade) were purchased from Sigma (St. Louis, MO, USA). TEMED was obtained from Promega (Madison, WI, USA). Dithiothreitol (DTT), acrylamide, methylenebisacrylamide, CHAPS, Clean-up kit, 2D Quant kit were obtained from Amersham Biosciences-GE Healthcare (Uppsala, Sweden). Immobiline pH-gradient (IPG) strip (pH 4–7), pharmalyte (pH 4–7), IPG buffer (pH 4–7) were obtained from Bio-Rad. All other chemicals and solvents were of the highest purity available.

Cell culture and MTT assay

For routine maintenance, A549 cells were cultured in suspension in RPMI-1640 media with 20% fetal bovine serum (GIBCO), 100 μg/mL penicillin and 10 μg/mL streptomycin (GIBCO) in a water-jacketed 5% CO_2 incubator at 37°C (Forma Scientific, Marietta, OH).

Drug sensitivity was evaluated using a standard colorimetric MTT assay. Briefly, cells in logarithmic growth phase were plated in 96-well microtitre plates at a density of 3×10^3–10^4 cells/100 μl per well and allowed to incubate 24 h at 37°C for attachment. Subsequently, purified R-MVL protein sample was diluted with complete medium to the desired initial concentration and then added to cells of the logarithmic phase. After incubation for another 72 h, the MTT solution (Bornem, Belgium) (20 μl of 5 mg/ml) was added to each well, then for additional 4 h incubation at 37°C. MTT-containing medium was removed and the formazan crystals, formed within the cells, were solubilized by the addition of DMSO (Bornem, Belgium) (150 μl/well) and agitation. The absorbance of the samples and control cultures were read at 570 nm with a spectrophotometer (Model 3550 Microplate Reader). The half inhibition rate IC50 was calculated. Each of cell lines was administrated to various concentration of R-MVL in triplicate, and each experiment was repeated three times.

Morphology and flow cytometry analysis of R-MVL-treated A549 cells

The cellular morphology was observed using phase contrast microscopy (Leica, Wetzlar, Germany). Apoptotic nuclear morphology was assessed using Hoechst 33342/PI (St. Louis, MO, USA). After being treated with R-MVL (8–64 μg/ml) and induced for 72 h, the culture medium was sucked from culture plates, and the cells were fixed with 3.7% paraformaldehyde for 30 min at room temperature. Subsequently, the fixed cells were rinsed with PBS three times and stained with Hoechst 33258/PI at 37°C for 30 min. After decanting the staining solution, the cells were rinsed with PBS three times, then the culture plates were placed under fluorescent microscope (Olympus, Tokyo, Japan) so that cellular nuclear damage was observed.

Flow cytometry was introduced to further investigate cells apoptosis effect by R-MVL. The cells were seeded in 100 mm culture dishes at a density of 2×10^6 and allowed to attach overnight. The medium was replaced with fresh complete medium containing the desired concentration of R-MVL, and the cells were incubated at 37°C for 72 h followed by harvest by centrifugation ($200 \times g$, 5 min). The collected cells were washed with cold phosphate-buffered saline (PBS) for three times and fixed in cold 75% ethanol at 4°C for 24 h. After that, the cells were rinsed with PBS two times and mixed with equal volume of double staining solution [Annexin V-FITC and PI, 50 μg/ml RNase and 0.1% (w/v) Triton X-100 in sodium citrate (3.8 mM)].

Apoptosis were measured using a FACSCalibur flow cytometer (Becton–Dickinson, Franklin Lakes, NJ, USA). The percentages of apoptotic (annexin+/PI−) and necrotic (annexin+/PI+) cells were determined with Cell Quest Pro software.

Proteomic sample preparation

Cultured cells were washed three times in ice-cold PBS (137 mM NaCl, 2.7 mM KCl, 10 mM Na_2HPO_4, 2 mM KH_2PO_4, pH 7.4) after removal of medium. Then cells were directly disrupted in 300 µl of a lysis buffer (7 M urea, 4% CHAPS, 2 M thiourea, 30 mM Tris, pH 8.8) containing 1% protease inhibitors, 50 µg/ml RNase, and 200 µg/ml DNase. After pelleting the insoluble material by centrifugation at 15,000×*g* for 30 min at 4°C, the supernatant was collected. According to the manufacture's instructions, the protein samples were cleaned up and quantified with Clean-up kit and 2D Quant Kit.

Two-dimensional gel electrophoresis

For the first dimensional isoelectric focusing (IEF), the protein solutions (450 µg) were directly applied onto IPG strips (24 cm, pH 4–7, linear), and rehydrated at 17°C and 50 V for 12 h. After rehydration, isoelectric focusing was carried out using a Bio-Rad PROTEAN IEF cell (Bio-Rad) and focusing was conducted by stepwise increase of the voltage as follows: the initial voltage was held at 250 V for 30 min; in the second step was quickly increase from 250 to 1,000 V within 60 min; in the third step was linearly increased from 1,000 to 10,000 V within 5 h; for the last step it was maintained at 500 V for 10 h. The plate temperature was maintained at 20°C during isoelectric focusing. After IEF separation, each IPG strip was incubated in equilibration buffer I (50 mM Tris–HCl, pH 8.8, 6 M urea, 2% SDS, 30% glycerol, 1% DTT) for 20 min with gently agitation, followed by incubation in buffer Π (50 mM Tris–HCl, pH 8.8, 6 M urea, 2% SDS, 30% glycerol, 2.5% IAA) for 15 min with gently agitation. IPG strips were then rinsed with SDS-PAGE running buffer and were directly loaded onto 11–17% linear acrylamide gradient gels. Subsequently, strips were overlayed with agarose solution [60 mM Tris–HCl pH 6.8, 60 mM SDS, 0.5% (w/v) agarose, 0.01% (w/v) bromophenol blue]. The second dimensional separation was performed in two steps at 10°C: 15 mA/gel for 30 min and 30 mA/gel until the bromophenol blue dye front reached the bottom of the gel. Then SDS-PAGE gels were washed with deionized water three times 15 min each and stained for at least 12 h with Coomassie Brilliant Blue G-250 (20% colloidal Coomassie ethanol, 1.6% phosphoric acid, 8% ammonium sulfate, 0.08% Coomassie Brilliant Blue G-250). Three replicates were run for the samples.

2-DE image analysis

The 2-D gel images were scanned using a Typhoon laser scanner (GE Healthcare, Uppsala, Sweden) at the resolution of 100 µm and analyzed using PDQuest package software version 7.1.1 (Bio-Rad, Hercules, CA, USA). Spot detection, background subtraction and spot quantitation were performed on 16-bit TIEF images acquired with a scanning densitometer. The protein spot volume was measured according to the lowest boundary mode of background selection. The spot volumes were normalized according to the total spot volume for each gel. Protein spot intensity was defined as the normalized spot volume which is the ratio of the single spot volume to the total spots volumes on a 2-D gel. The computer analysis allowed automatic detection and quantification of protein spots, as well as matching between control gels and gels from treated samples. The significance of differences of protein spots were evaluated by Student's *t* test and $p < 0.05$ was considered as significant.

In-gel tryptic digestion

The protein changed spots were manually excised and transferred to 500 µL siliconized Eppendorf tubes. Subsequently, the gel plugs destained twice with freshly prepared 200 µL of 50% (v/v) acetonitrile/25 mM ammonium bicarbonate buffer and incubated at room temperature (25°C). The gel plugs were then washed once with 200 µL of 100% ACN for 5 min at room temperature and dried in a Speed Vac Plus SC110A (Savant, Holbrook, NY, USA) vacuum concentrator. After the plugs had dried completely, 20 µL of 25 mM ammonium bicarbonate containing 5 ng of sequencing grade modified trypsin solution (Promega, Madison, WI) was added and the samples incubated at 37°C for at least 16 h for complete digestion (Shevchenko et al. 1996). Peptides were extracted from the gel plugs with 50 µL of 50% (v/v) ACN/1% (v/v) TFA and agitation in a shaker (140 rpm) for 15 min. Tryptic peptides were collected, dried, and resuspended in 4 µL of 20% ACN/0.1% TFA for MS analysis.

Protein identification

Equal volumes of trypsinized samples (0.5 µl) and the matrix solution (0.5 µl) containing 5 mg/ml α-cyano-4-hydroxycinnamic acid (Sigma–Aldrich Fluka, St. Louis, MO) prepared in 50% ACN, 0.1% v/v TFA and 2% w/v ammonium citrate. The samples/matrix mixture was then spotted onto the 96-well MALDI-TOF MS target plate. Peptide extracts were analyzed on a MALDI-TOF–MS

(Autoflex III, Bruker Daltonik, Bremen, Germany) in the positive ion reflectron mode. We used a protein molecular mass range of 6–200 kDa and a mass tolerance of 100 ppm for the internal calibration. For protein identification, we performed database searching against the NCBInr database using the MASCOT program and the MASCOT search engine with the following parameters: (1) Swiss-Prot, 2006 Database (http://www.us.expasy.org/sprot); (2) molecular weight (MW) of protein; (3) isoelectric point (pI); (4) one missed cleavage; (5) fixed modifications, carbamidomethylation (C); (6) variable modifications, oxidation (M). The expectation value (chance of misidentification) is less than 0.05.

Bioinformatics analysis

The molecular function and biological process of differentially expressed proteins were defined by PANTHER (Proteins Through Evolutionary Relationships) (Thomas et al. 2003). Protein–protein interaction networks were built on PPI Spider (Antonov et al. 2009) and i2d (Brown and Jurisica 2007).

Results

R-MVL induces apoptosis in A549 cells

The MTT measurement results showed that R-MVL (2–64 μg/ml) can exert a remarkable inhibitory effect on the growth of A549 cells. Treating the cells with R-MVL (2–64 μg/ml) resulted in a dose-dependent inhibition of cellular proliferation. The IC50 value of R-MVL in A549 cells was estimated to be 24.12 μg/ml.

In morphology analysis, cell nucleus structure was intact and homogeneously slightly stained by Hoechst 33342 for the negative control (Fig. 1a). However, the R-MVL (8–64 μg/ml) treatment groups were significantly different, in which nuclear condensation, cells nucleus diffusion and apoptotic cell appeared. In another negative control (Fig. 1b), the living cells and apoptotic cells was also slightly stained by PI. When R-MVL was increased from 8 to 64 μg/ml, the cells were mightily stained and necrotic death cell was increased by fluorescence microscope. Moreover, compared with the negative control group, round detached cells and reduced cell density were gradually increased by phase contrast microscopy. The morphology structure of A549 cells treated with R-MVL (8–64 μg/ml) exhibited characteristics of apoptosis such as cell membrane shrinkage, condensation and fragmentation of nuclear chromatin and formation of apoptotic bodies (Fig. 1c). Together, these results suggested that R-MVL could induce apoptosis and necrotic death of A549 cells.

To further investigate the underlying mechanism of the anti-proliferative activity, we performed flow cytometric analysis. Based on the characteristic of apoptotic cells, unaffected cells, early apoptotic cells, and late apoptotic cells were distinguished by double staining of cells with Annexin V-FITC and PI. In the MVL-treated A549 cells for 72 h with 8, 32 and 64 μg/ml, the percentage of apoptotic tumor cells were found to be 18.61, 21.28 and 81.93%, respectively (Fig. 1d). Thus, flow cytometric analysis also shows that R-MVL reduces proliferation of A549 cells by inducing apoptosis and necrotic death in a dose-dependent manner.

2-DE gel comparison

In order to compare the protein expression profiles of A549 cells with and without R-MVL treatment, samples of 450 μg protein were directly extracted with the urea lysis solution and separated by 2D-PAGE, the results are shown in Fig. 2a, b. To obtain statistically significant results, each protein sample was run in triplicate. The proteomic maps of MVL-treated cells and control were compared using PDQuest program to identify the protein spot variations. As a result, 50 protein spots were detected, which are significantly differentially expressed protein spots ($p < 0.05$) with twofold or more increased or decreased intensity as observed in all three replicate gels, after MVL treatment (Fig. 2c). Of them 35 protein spots were upregulated, and 15 downregulated.

Protein identification

Of the 50 differentially expressed proteins after R-MVL treatment, 10 of the interest spots (Fig. 2d, e) were excised manually, digested and finally identified by peptide mass fingerprinting using MALDI-TOF–MS/MS followed by database search. Consequently, seven protein spots were identified successfully, of which two were upregulated and five were downregulated. Table 1 shows their detailed information including protein MW/p*I*, SWISS-Prot accession numbers, Mascot Score, numbers of peptides matched, and coverage (percentage of predicted protein sequence covered by matched peptides). In MVL-treated A549 cells, two increased proteins were aldehyde dehydrogenase 1 family member A1 (ALDH1A1) and β-actin (ACTB), and five decreased proteins include: heat shock protein 90 kDa beta member 1 (HSP90B1), heat shock 60 kDa protein 1 (HSPD1), plastin 3 (Plastin 3), tropomyosin 3 isoform 2 (TPM3), and β-tubulin (TUBB). Based on PANTHER classification system, the identified 7 proteins can be classified into 3 functional categories: protein folding (HSP90, HSP60), cell structure and motility (ACTB, PLS3, TUBB and TPM3), and other carbon metabolism (ALDH1A1).

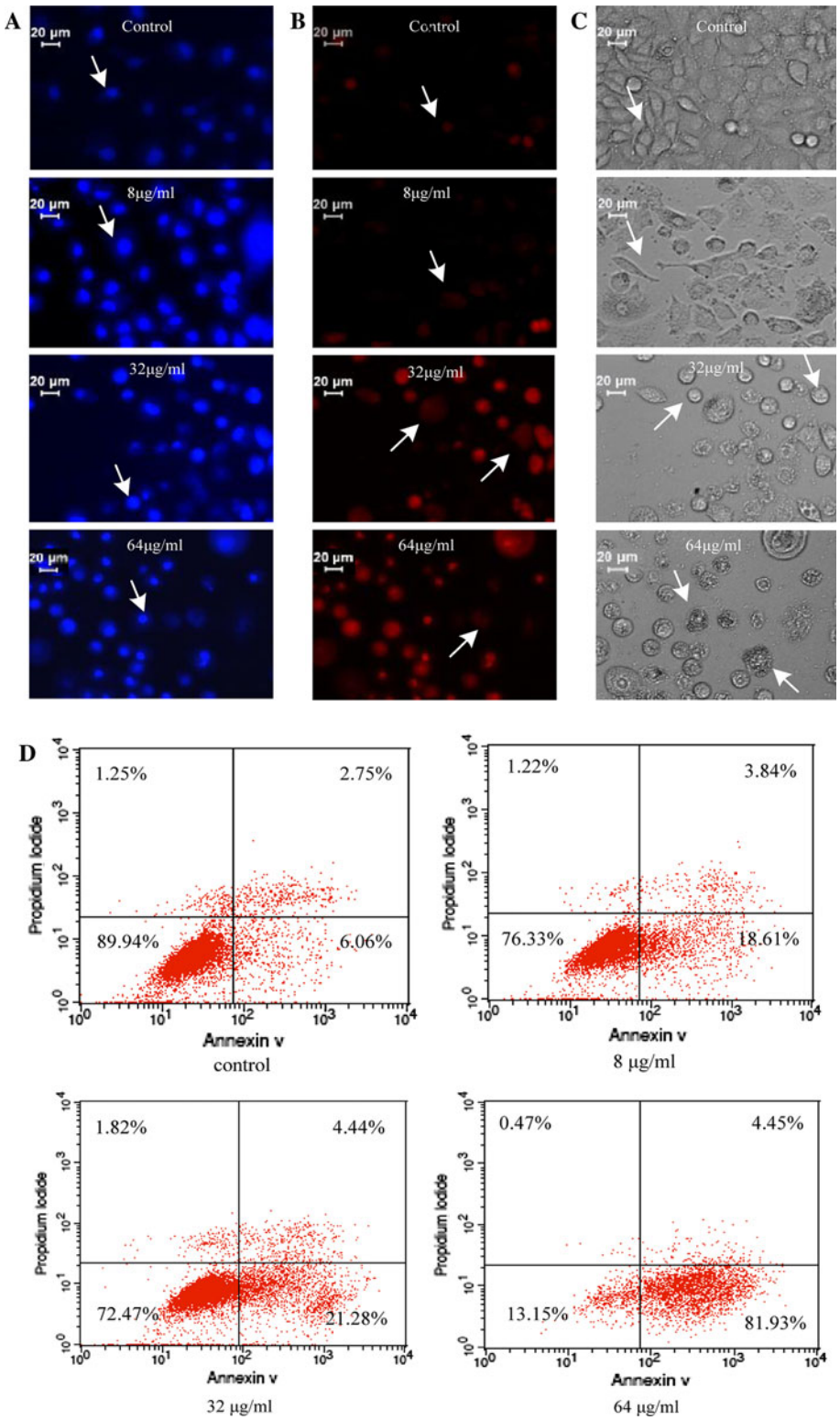

Fig. 1 R-MVL induces apoptotis in A549 cells. **a–c** R-MVL-induced morphologic changes in A549 cells observed by fluorescent microscopy and phase contrast microscopy. **a** Heochest stained, **b** PI stained, **c** phase contrast microscopy. **d** Apoptosis analysis of A549 cells by R-MVL using FACS with Annexin V-FITC and PI staining

Their functions include: chaperone (HSP90, HSP60), actin and actin binding protein (ACTB, PLS3, TPM3), tubulin (TUBB), as well as dehydrogenase (ALDH1A1) (Table 1). A representative MALDI-TOF–MS peptide mass fingerprint of spot 10 (tubulin-beta) is shown in Fig. 3.

Protein–protein interaction network analysis for the identified proteins

To explore the underlying pathways of apoptosis in A549 cells induced by recombinant MVL, protein–protein

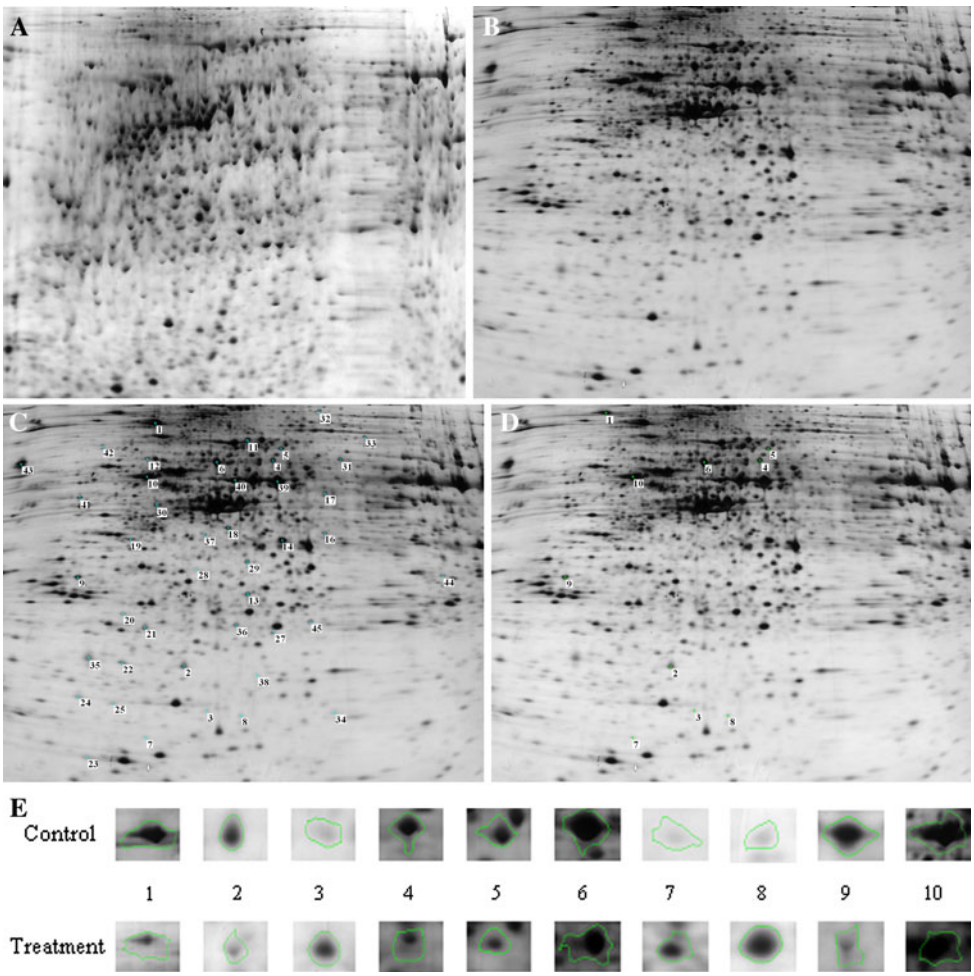

Fig. 2 2D gel proteome map from A549 cells with molecular weight and pH indicated on the *left* and head of the 2-DE gels, respectively. The labeled cell proteins were mixed and subjected to 24 cm pH 4–7 IEF electrophoresis followed by SDS-PAGE isolation. The gels were stained with Coomassie blue G-250 and the synthetic gel images were generated using PDQUEST program. **a** Image of proteins from A549 cells administrated without R-MVL. **b** Image of proteins from A549 cells administrated with R-MVL. **c** Differentially expressed 50 protein spots indicated by *numbers*. **d** Ten of the interest proteins are numbered from 1 to 10 and identified with the help of MALDI-TOF MS. **e** Ten of the interest protein spots are enlarged with *curve lines*. Numbers in the image correspond to the identified proteins described in Table 1

Table 1 The identified proteins with differential expressions in A549 cells treated by recombinant MVL

Spot no.	SWISS-Prot accession no.	Protein identified (function, category)	MW (Da)/p*I*[a]	Mascot score[b]	Matched peptides[c]	Coverage (%)[d]	Difference[e]
1	P14625	HSP90-β-1 (Hsp 90 family chaperone, protein folding)	9,269/4.76	339	5	8	−2.78
3	P60709	Actin-β (Actin and actin-related protein, cell structure)	4,730/5.3	262	4	9	4.15
5	P13797	Plastin 3 (non-motor actin binding protein, cell structure)	71,279/5.41	128	23	37	−2.94
6	P10809	HSP60 (chaperonin, protein folding)	6,120/5.70	619	5	14	−2.53
8	P00352	Aldehyde dehydrogenase (dehydrogenase, other carbon metabolism)	2,558/5.95	158	2	10	3.18
9	P06753	Tropomyosin 3 (actin binding motor protein, cell structure)	29,243/4.75	390	5	19	−2.56
10	P07437	Tubulin-β (tubulin, cell structure)	5,000/4.78	671	7	12	−3.86

A representative MALDI-TOF–MS peptide mass fingerprint spectrum for spot 10 was shown in Fig. 3a

[a] Observed MW and p*I* of protein spot in the 2-D gel

[b] Protein score greater than 79 is significant ($p < 0.05$)

[c] Number of peptides that match the predicted protein sequence

[d] The ratio of the protein sequence covered by the matched peptides

[e] Ratio of spot density (R-MVL-treated group/control)

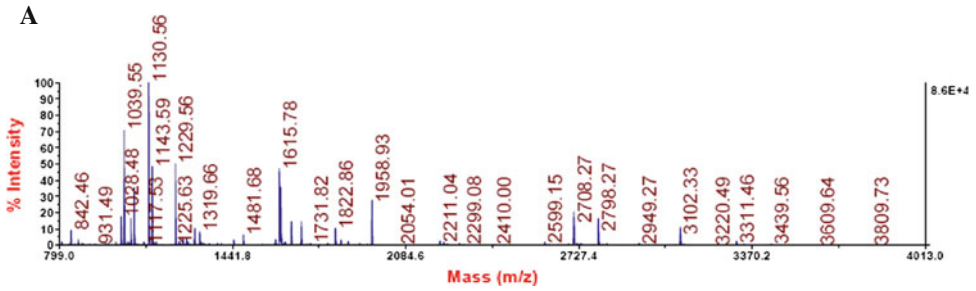

B

1 MREIVHIQAG QCGNQIGAKF WEVISDEHGI DPTGTYHGDS DLQLDRISVY

51 YNEATGGKYV PR**AILVDLEP** **GTMDSVR**SGP FGQIFRPDNF VFGQSGAGNN

101 WAK**GHYTEGA** **ELVDSVLDVV** **R**KEAESCDCL QGFQLTHSLG GGTGSGMGTL

151 LISKIREEYP DRIMNTFSVV PSPKVSDTVV EPYNATLSVH QLVENTDETY

201 CIDNEALYDI CFRTLK**LTTP** **TYGDLNHLVS** **ATMSGVTTCL** **RFPGQLNADL**

251 R**KLAVNMVPF** **PR**LHFFMPGF APLTSRGSQQ YRALTVPELT QQVFDAKNMM

301 AACDPRHGR**Y** **LTVAAVFR**GR MSMKEVDEQM LNVQNKNSSY FVEWIPNNVK

351 TAVCDIPPRG LKMAVTFIGN STAIQELFKR **ISEQFTAMFR** RKAFLHWYTG

401 EGMDEMEFTE AESNMNDLVS EYQQYQDATA EEEEDFGEEA EEEA

Fig. 3 A representative MALDI-TOF MS peptide mass fingerprint obtained for tryptic peptides eluted from 2-D gel spot 10. The *x*-axis represents mass-to-charge ratio (*m/z*), whereas the *y*-axis represents relative abundance. **a** The MALDI-TOF mass spectrum of *β*-tubulin, **b** the matched peptide sequences are marked with **black body**

interaction network analysis was performed on the seven identified proteins. Firstly, PPI spider was employed and six of the seven identified proteins, except for ALDH1A1, can be mapped a protein–protein interaction sub-network (Fig. 4a). In this network, several interacting proteins were introduced: HLA-B (major histocompatibility complex, GeneID: 3106), IKBKE (inhibitor of kappa light polypeptide gene enhancer in B cells, kinase epsilon, GeneID: 9641), 14-3-3 zeta (tyrosine 3-monooxygenase/tryptophan 5-monooxygenase activation protein, zeta polypeptide, GeneID: 7534), GRB2 (growth factor receptor-bound protein 2, GeneID: 2885), HSP90AB1 [heat shock protein 90 kDa alpha (cytosolic), class B member 1, GeneID: 3326], CFTR (cystic fibrosis transmembrane conductance regulator, GeneID: 1080), CHUK (conserved helix–loop–helix ubiquitous kinase, GeneID: 1147). Notably, among the seven identified proteins, four proteins (downregulated HSP90, HSP60 and tubulin-beta, upregulated actin-beta) are the direct interactors of 14-3-3 zeta, suggesting that 14-3-3 zeta may play a vital role in mediating MVL-induced apoptosis in lung cancer cells.

Furthermore, i2d database was used to search protein association network for the identified proteins. All the seven identified proteins were mapped to a complex protein network (Fig. 4b): 2 interactions for ALDH1A1, 31 interactions for TPM3, 46 interactions for tubulin-beta, 125

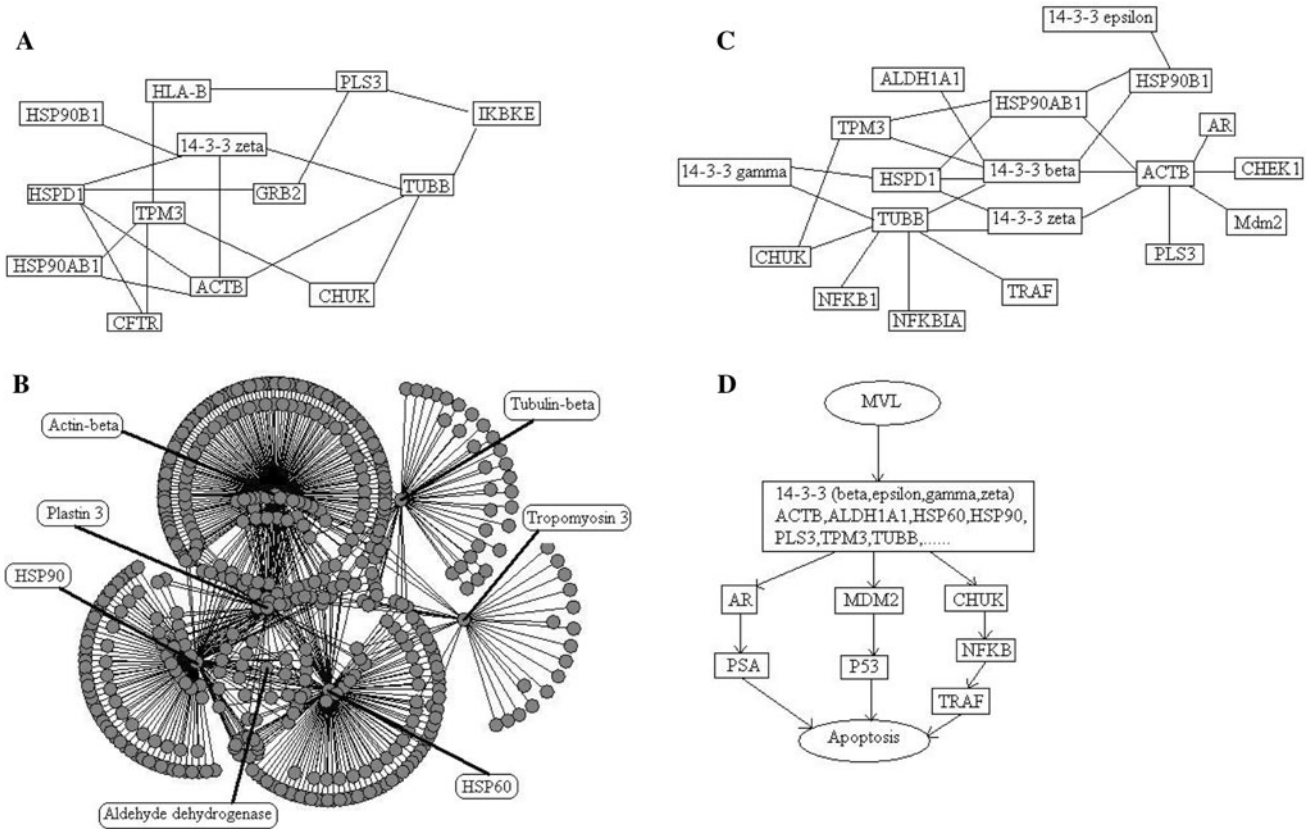

Fig. 4 **a** Protein–protein interaction networks built on KEGG spider for the identified proteins, **b** protein–protein interaction networks built on i2d for the identified proteins, **c** a subset extracted from **b**, **d** predicted apoptotic pathways for R-MVL treatment in A549 cells

interactions for HSP60, 73 interactions for plastin-3, 121 for HSP90, and 199 interactions for actin-beta. A subnetwork was extracted from such a complex network (Fig. 4c). Some interacting proteins were introduced: TRAF1 (TNF receptor-associated factor 1, GeneID: 7185), AR (androgen receptor, GeneID: 367), Mdm2 (p53 binding protein homolog, GeneID: 4193), and several 14-3-3 proteins (zeta, GeneID: 7534; beta, GeneID: 7529; gamma, GeneID: 7532; epsilon, GeneID: 7531). Interestingly, among the seven identified proteins, six proteins (upregulated actin-beta and ALDH1A1, downregulated HSP90, HSP60, tubulin-beta and TPM3) are the direct interactors of 14-3-3 beta, meaning that 14-3-3 beta could be very important mediator in MVL-induced apoptosis in lung cancer cells.

Together, by network analysis, some important proteins having interactions with the identified seven proteins were identified, for example, GRB2, CHUK, TRAF1, MDM2, AR, and four 14-3-3 proteins (beta, epsilon, gamma, zeta). In particular, among the seven identified proteins, four or six proteins are the direct interactors of 14-3-3 zeta or 14-3-3 beta, respectively, suggesting their important role in mediating MVL-induced apoptosis in lung cancer cells.

Discussion

To date, studies in MVL are focused on its anti-HIV activity. This study is the first to investigate its antitumor activity, especially, is the first to employ proteomic technique to globally search for the dysregulated proteins induced by plant lectins in human cancer cells (to our knowledge, in other proteomic studies, plant lectins are generally used as the protein-capture reagents like lectin-column only).

In the present work, we firstly assessed the anti-cancer activity of R-MVL in A549 cells by using FM and FCM, and found that R-MVL induces apoptosis in A549 cells in a dose-dependent manner. As a desirable end point for cancer therapy, apoptosis induction was probably the most potent defense against cancer (Hengartner 2000; Meier et al. 2000; Liu et al. 2008), this makes R-MVL be potent anti-cancer candidate agent. Subsequently, a proteomic approach (2-DE, image analysis, and mass spectrometry with protein database interrogation strategies) was introduced to investigate protein expression patterns of A549 cells in response to R-MVL treatment. Fifty protein spots with twofold or more alterations were detected, ten spots were excised from the 2-D gels and seven differentially

expressed proteins were successfully identified by MALDI-TOF–MS/MS followed by database search, including five downregulated (HSP90, HSP60, β-tubulin, plastin 3, tropomyosin 3) and two upregulated (aldehyde dehydrogenase and β-actin).

Furthermore, bioinformatic analysis was employed to infer the protein networks associated with the identified seven proteins. Among them there are some very interesting interactors, including GRB2, CHEK1, CHUK, NFKBIA, NFKB1, TRAF1, MDM2, AR, PSA, and four 14-3-3 proteins (beta, epsilon, gamma, zeta). In particular, among the seven identified proteins, four or six proteins are the direct interactors of 14-3-3 zeta or 14-3-3 beta, respectively, suggesting that the two proteins could play very important role in MVL-induced apoptosis in A549 cells. In fact, 14-3-3 proteins have emerged as critical regulators of diverse cellular processes, including signal transduction, apoptosis, cell cycle progression and DNA replication. The highly conserved human 14-3-3 gene family encodes proteins with either tumor-promoting or tumor-suppressing activities. The crucial point for the proper functioning of cells is the cellular balance between the various 14-3-3 isoforms (Niemantsverdriet et al. 2008). The plasma levels of 14-3-3 sigma, beta, and eta in the lung cancer patients were significantly lower than those in the control subjects (Xiao et al. 2005). The increased 14-3-3 zeta expression was positively correlated with a more advanced pathologic stage and grade of non-small cell lung cancers (Fan et al. 2007). The decreased 14-3-3 zeta suppresses anchorage-independent growth of lung cancer cells through anoikis activation (Li et al. 2008a).

Finally, in order to find some clues about how these interactors specifically mediate MVL to induce apoptosis of A549 cells, we searched these interactors in the cancer pathway map provided by KEGG database (map09020) and found that there are several routes to apoptosis endpoint: (1) CHUK—NFKBI—NFKB—TRAF—apoptosis; (2) MDM2—p53—apoptosis; (3)AR—PSA— apoptosis. Thus, combining them with the results of network analysis, three potential pathways for MVL-induced apoptosis in lung cancer cells could be predicted (Fig. 4d). We speculated that the inhibitions of these pathways might represent several new strategies for treating lung cancer; future work will test these predictions.

Conclusions

In the present study, for the first time, we investigated the anti-cancer activity of R-MVL in A549 cells and characterized the changes on proteome of A549 cell differentiation induced by R-MVL. Seven differentially expressed proteins were identified. In particular, our bioinformatics analysis suggested that 14-3-3 zeta or 14-3-3 beta could play a vital role in MVL-induced apoptosis in A549 cells, and predicted three potential apoptotic pathways triggered by this anti-cancer agent: AR/PSA pathway, MDM2/p53 pathway and CHUK/NFKB pathway. These findings provide clues for the development of novel therapeutic strategies by interfering with the functions of some proteins in these pathways such as 14-3-3 (beta, zeta) or MDM2 or NFKB or AR proteins.

Conflict of interest The authors declare that they have no conflict of interest.

References

Antonov AV, Dietmann S, Rodchenkov I, Mewes GW (2009) PPI spider a tool for the interpretation of proteomics data in the context of protein–protein interaction networks. Proteomics 9:2740–2749

Brown KR, Jurisica I (2007) Unequal evolutionary conservation of human protein interactions in interologous networks. Genome Biol 8(5):R95

Fan T, Li RY, Todd NW, Qiu Q, Fang HB, Wang HJ, Shen JJ, Zhao RY, Caraway NP, Katz RL, Stass SA, Jiang F (2007) Up-regulation of 14–3-3 zeta in lung cancer and its implication as prognostic and therapeutic target. Cancer Res 67(16):7901–7906

Greenlee RT, Murray T, Bolden S, Wingo PA (2000) Cancer statistics, 2000. CA Cancer J Clin 50(1):7–33

Gridelli C, Rossi A, Maione P (2003) Treatment of non-small-cell lung cancer: state of the art and development of new biologic agents. Oncogene 22(42):6629–6638

Hengartner MO (2000) The biochemistry of apoptosis. Nature 407(6805):770–776

Kim JH, In YJ, Kim WK, Bae KH, Kang S, Lee SC (2008) Differential signatures of protein glycosylation and phosphorylation in human Chang liver cells induced by TCDD treatment. Toxicol Lett 178(1):20–28

Li ZG, Zhao J, Du YH, Park HR, Sun SY, Bernal-Mizrachi L, Aitken A, Khuri FR, Fu HA (2008a) Down-regulation of 14–3-3 zeta suppresses anchorage-independent growth of lung cancer cells through anoikis activation. Proc Natl Acad Sci USA 105(1):162–167

Li YQ, Zhang XW, Chen G, Wei D, Chen F (2008b) Algal lectins for potential prevention of HIV transmission. Curr Med Chem 15:1096–1104

Liu Z, Liu B, Zhang ZT, Zhou TT, Bian HJ, Min MW, Liu YH, Chen J, Bao JK (2008) A mannose-binding lectin from *Sophora flavescens* induces apoptosis in HeLa cells. Phytomedicine 15(10):867–875

Martinkova J, Gadher SJ, Hajduch M, Kovarova H (2009) Challenges in cancer research and multifaceted approaches for cancer biomarker quest. FEBS Lett 583(11):1772–1784

Meier P, Finch A, Evan G (2000) Apoptosis in development. Nature 407(6805):796–801

Niemantsverdriet M, Wagner K, Visser M, Backendorf C (2008) Cellular functions of 14-3-3 zeta in apoptosis and cell adhesion emphasize its oncogenic character. Oncogene 27(9):1315–1319

Pan XH, Liu X, Zhao BX, Xie YS, Shin DS, Zhang SL, Zhao J, Miao JY (2008) 5-Alkyl-2-ferrocenyl-6, 7-dihydropyrazolo(1, 5-a)pyrazin-4(5H)-one derivatives inhibit growth of lung cancer A549 cell by inducing apoptosis. Bioorg Med Chem 16(20):9093–9100

Shevchenko A, Wilm M, Vorm O, Mann M (1996) Mass spectrometric sequencing of proteins silver-stained polyacrylamide gels. Anal Chem 68(5):850–858

Thomas PD, Campbell MJ, Kejariwal A, Mi H, Karlak B, Daverman R, Diemer K, Muruganujan A, Narechania A (2003) PANTHER: a library of protein families and subfamilies indexed by function. Genome Res 13:2129–2141

Williams DC, Lee JY, Cai ML, Bewley CA, Clore GM (2005) Crystal structures of the HIV-1 inhibitory cyanobacterial protein MVL free and bound to Man3GlcNAc2. J Biol Chem. 280:29269–29276

Xiao T, Ying WT, Li L, Hu Z, Ma Y, Jiao LY, Ma JF, Cai Y, Lin DM, Guo SP, Han NJ, Di XB, Li M, Zhang DC, Su K, Yuan JS, Zheng HW, Gao MX, He J, Shi SS, Li WJ, Xu NZ, Zhang HS, Liu Y, Zhang KT, Gao YN, Qian XH, Cheng SJ (2005) An approach to studying lung cancer-related proteins in human blood. Mol Cell Proteomics 4(10):1480–1486

Yamaguchi M, Ogawa T, Muramoto K, Kamio Y, Jimbo M, Kamiya H (1999) Isolation and characterization of a mannan-binding lectin from the freshwater Cyanobacterium (blue-green algae) *Microcystis viridis*. Biochem Biophys Res Commun 265:703–708